2011-09

From conformal invariance to quasistationary states

Journal of Statistical Mechanics, Bristol : Institute of Physics - IOP, v. 2011, p. P09030-1-P09030-21, Sept. 2011

http://www.producao.usp.br/handle/BDPI/49630

From conformal invariance to quasistationary states

J. Stat. Mech. (2011) P09030

(http://iopscience.iop.org/1742-5468/2011/09/P09030)

Journal of Statistical Mechanics: Theory and Experiment
An IOP and SISSA journal

From conformal invariance to quasistationary states

Francisco C Alcaraz[1] **and Vladimir Rittenberg**[2]

[1] Instituto de Física de São Carlos, Universidade de São Paulo, Caixa Postal 369, 13560-590, São Carlos, SP, Brazil
[2] Physikalisches Institut, Universität Bonn, Nussallee 12, 53115 Bonn, Germany
E-mail: alcaraz@if.sc.usp.br and vladimir@th.physik.uni-bonn.de

Received 13 July 2011
Accepted 1 September 2011
Published 30 September 2011

Online at stacks.iop.org/JSTAT/2011/P09030
doi:10.1088/1742-5468/2011/09/P09030

Abstract. In a conformal invariant one-dimensional stochastic model, a certain nonlocal perturbation takes the system to a new massless phase of a special kind. The ground-state of the system is an adsorptive state. Part of the finite-size scaling spectrum of the evolution Hamiltonian stays unchanged but some levels go exponentially to zero for large lattice sizes, becoming degenerate with the ground-state. As a consequence one observes the appearance of quasistationary states which have a relaxation time which grows exponentially with the size of the system. Several initial conditions have singled out a quasistationary state which has in the finite-size scaling limit the same properties as the stationary state of the conformal invariant model.

Keywords: driven diffusive systems (theory), phase transitions into absorbing states (theory), stochastic particle dynamics (theory), metastable states

J. Stat. Mech. (2011) P09030

1742-5468/11/P09030+21$33.00

Contents

1. Introduction

We have recently [1] presented the peak adjusted raise and peel model (PARPM). This is a one-parameter (denoted by p) extension of the well studied, raise and peel (RPM) one-dimensional growth model [2, 3]. The latter model is recovered if one takes $p = 1$. The PARPM is defined in the configuration space of Dyck (restricted solid-on-solid, RSOS) paths on a lattice with $L + 1$ sites (L even). The RSOS configurations can be seen as an interface separating a fluid of tiles covering a substrate and a rarefied gas of tiles hitting the interface. If $h(i)$ $(i = 0, 1, \ldots, L)$ is the height at the site i of an RSOS path, for the substrate one has $h(2k) = 0, h(2k + 1) = 1$. The interface is composed of clusters which touch each other. Depending on the position of the hit, the tile can be locally adsorbed (increasing the size of a cluster or fusing two clusters) or can trigger a nonlocal desorption, peeling part of a layer of tiles from the surface of a cluster. With a p-dependent probability, a tile hits a peak (local maximum) and is reflected. The other sites are hit with equal probabilities. The effective rates for adsorption and desorption become dependent on the total number of peaks of the configuration, on the size L of the system, and on p.

If the parameter $p = 1$, the rates are all equal to 1 and independent of the number of peaks and the size L of the system. The situation is very different if $p \neq 1$. The dependence of the rates on the global properties of the configuration can be seen as a process with long-range interactions. The larger the value of the parameter p $(p > 1)$, the stronger the 'long-range' effect is. Configurations with many peaks become more stable. The slowing down of configurations with many peaks will lead us to new physics.

It was shown in [1] that for $0 \leq p \leq p_{\max}$, where $p_{\max} = 2(L - 1)/L$, in the finite-size scaling limit, the properties of the system are p independent. The system is conformal invariant (this is the merit of the model) and the stationary states have many well understood properties. The p dependence of the model appears only in the non-universal sound velocity $v_s(p)$ which fixes the time scale. The spectra of the Hamiltonians describing

J. Stat. Mech. (2011) P09030

the time evolution of the system are given by a known representation of the Virasoro algebra [4]. Moreover it was observed that if $p = p_{\max}$ the stationary state becomes an absorbing state, i.e. with probability 1 one finds only one configuration. This is a new phase. The absorbing state corresponds to the configuration given by the substrate (maximum number of peaks). Conformal invariance should be lost. It turns out that the picture is much more complex, and the PARPM at $p = p_{\max}$ has fascinating properties. One observes quasistationary states (QSSs), and conformal invariance is broken in an uncanny way. One should keep in mind that one is dealing with a nonlocal model. For $p > p_{\max}$ some rates become negative and the stochastic process is ill defined.

The present paper deals only with the new phase of the PARPM and is a natural continuation of our previous work [1]. The presentation of the model in section 2 in this paper is a mere repetition of section 2 of [1].

Since except for $p = 1$ the PARPM is not integrable, we have studied its properties using Monte Carlo simulations on large systems (up to $L = 70\,000$). For the study of the spectrum of the evolution Hamiltonian we have done numerical diagonalizations of lattices up to $L = 18$ sites and up to $L = 30$ for one special case.

In section 3, using Monte Carlo simulations we study the time evolution of the system. We show that, surprisingly, for moderate system sizes and various initial conditions, after a short transient time the system stays practically unchanged for a long relaxation time in a QSS.

QSSs are observed in systems with long-range or mean-field interactions in statistical mechanics and Hamiltonian dynamics. There is a long list of papers on this subject and we refer the reader to some reviews [5, 6]. For the effects of noise on the existence of QSS, see [7]. Typically the time the system spends in a QSS increases with the length of the system following a power law. Exponentially divergent transient times were observed in cellular automata and in coupled map lattices [8, 9]. We are aware of only one other stochastic model defined on a lattice (the ABC model [10]) in which QSSs are seen. In this model in the stationary state translational invariance is broken. The sites are occupied in alphabetical order by three blocks of A, B or C particles. In the QSSs there are more blocks. As we are going to see, our model is very different.

In order to understand the origin of QSSs, in section 4 we perform a finite-size scaling study of the spectra of the Hamiltonian which gives the time evolution of the system. In the unperturbed ($p < p_{\max}$) case, the finite-size scaling spectrum is given by the conformal dimensions Δ. They are equal to all non-negative integer numbers except 1 (there is no current). The degeneracies are also known [4].

It turns out that in the new phase all the properly scaled energy levels stay unchanged, except for one level for each even conformal dimension (this includes the energy–momentum tensor which plays a crucial role in conformal invariance and has $\Delta = 2$!). We are thus left with

$$\Delta = 0, 3, 4, \ldots, \tag{1.1}$$

with a degeneracy smaller by one unit for all even values of Δ starting with $\Delta = 4$. This is not a rigorously proven result but a conjecture based on numerics up to $\Delta = 7$.

If we increase the lattice size of the system, all the levels which are no longer in the conformal invariant towers go exponentially to zero. This makes the value $\Delta = 0$ infinitely degenerate in the infinite volume limit. One should keep in mind that the configuration

J. Stat. Mech. (2011) P09030

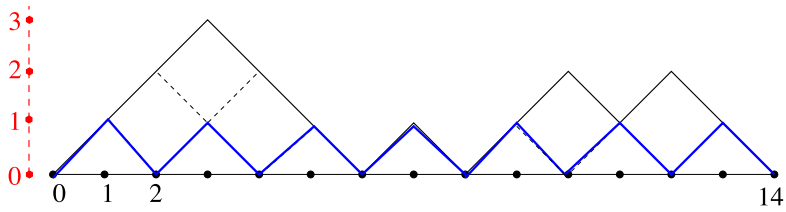

Figure 1. An example of a Dyck path for $L = 14$. There are four contact points and three clusters. The substrate profile is shown in blue.

corresponding to the substrate, which is an absorbing state, has also $\Delta = 0$. For finite volumes, the missing levels are the origin of the QSS.

In section 5, in order to make the connection between eigenfunctions and the probability distribution functions (PDF) seen in QSSs, we mention some properties of intensity matrices (the Hamiltonian is one of them) when one of the states is an absorbing state.

We next derive some properties of the QSS related to the eigenfunction of the energy level originally at $\Delta = 2$ for $p < p_{\max}$, and which decreases exponentially to the value $\Delta = 0$ at $p = p_{\max}$. This correspondence is possible due to a unique property of the eigenfunction of the first excited level of an intensity matrix in the presence of an absorbing state.

Using Monte Carlo simulations and initial conditions in which the probability of having the substrate is taken as zero, in section 6 we have studied the density of contact points and the average height in the finite-size scaling limit. If the system is conformal invariant, both these quantities are given by precise analytic expressions. It turns out that in the QSS state, with very high accuracy, the same expressions describe the data. This result is more than surprising. As we have discussed, in the new phase the finite-size scaling spectrum of the Hamiltonian (which gives the time-like correlation functions) is not the same as in the conformal invariant region and one would expect the space-like correlation functions to change too.

The open questions and our conclusions are presented in section 7.

2. Description of the peak adjusted raise and peel model

We consider an open one-dimensional system with $L + 1$ sites (L even). A Dyck path is a special RSOS configuration defined as follows. We attach to each site i non-negative integer heights h_i which obey RSOS rules:

$$h_{i+1} - h_i = \pm 1, \qquad h_0 = h_L = 0 \quad (i = 0, 1, \ldots, L-1). \tag{2.1}$$

There are

$$Z(L) = L!/(L/2)!(L/2+1)! \tag{2.2}$$

configurations of this kind. If $h_j = 0$ at site j one has a contact point. Between two consecutive contact points one has a cluster. There are four contact points and three clusters in figure 1.

J. Stat. Mech. (2011) P09030

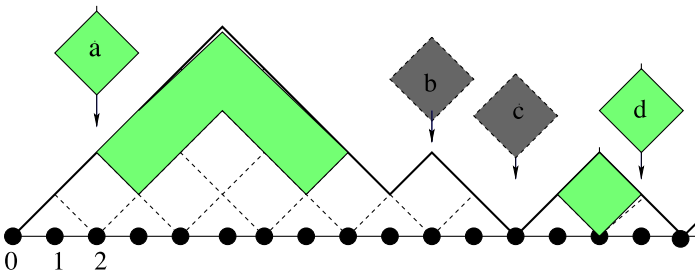

Figure 2. Example of a configuration with four peaks of the PARPM for $L = 18$. Depending on the position where the tilted tiles reach the interface, several distinct processes occur (see the text).

A Dyck path is seen as an interface separating a film of tilted tiles deposited on a substrate from a rarefied gas of tiles (see figure 2). The stochastic processes in discrete time has two steps:

(a) Sequential updating. With a probability $P(i)$ a tile hits the site $i = 1, \ldots, L-1$ ($\sum_i P(i) = 1$). In the RPM, $P(i)$ is chosen uniform: $P(i) = P = 1/(L-1)$. In the PARPM, this is no longer the case. For a given configuration c (there are $Z(L)$ of them) with n_c peaks all the peaks are hit with the same probability $R_p = p/(L-1)$ (p is a non-negative parameter), all the other $L-1-n_c$ sites are hit with the same probability $Q_c = q_c/(L-1)$. Since

$$n_c R_p + (L-1-n_c)Q_c = 1 \tag{2.3}$$

q_c depends on the configuration c and on the parameter p, and we have that

$$q_c = (L-1-pn_c)/(L-1-n_c), \qquad c = 1, 2, \ldots, Z(L). \tag{2.4}$$

(b) Effects of a hit by a tile. The consequence of the hit on a configuration is the same as in the RPM at the conformal invariant point. Depending of the slope $s_i = (h_{i+1} - h_{i-1})/2$ at the site i, the following processes can occur:

(1) $s_i = 0$ and $h_i > h_{i-1}$ (tile b in figure 2). The tile hits a peak and is reflected.

(2) $s_i = 0$ and $h_i < h_{i-1}$ (tile c in figure 2). The tile hits a local minimum and is adsorbed ($h_i \to h_i + 2$).

(3) $s_i = 1$ (tile a in figure 2). The tile is reflected after triggering the desorption ($h_j \to h_j - 2$) of a layer of $b-1$ tiles from the segment $\{j = i+1, \ldots, i+b-1\}$ where $h_j > h_i = h_{i+b}$.

(4) $s_i = -1$ (tile d in figure 2). The tile is reflected after triggering the desorption ($h_j \to h_j - 2$) of a layer of $b-1$ tiles belonging to the segment $\{j = i-b+1, \ldots, i-1\}$ where $h_j > h_i = h_{i-b}$.

The continuous time evolution of a system composed by the states $a = 1, 2, \ldots, Z(L)$ with probabilities $P_a(t)$ is given by a master equation that can be interpreted as an

doi:10.1088/1742-5468/2011/09/P09030

J. Stat. Mech. (2011) P09030

imaginary time Schrödinger equation:

$$\frac{\mathrm{d}}{\mathrm{d}t}P_a(t) = -\sum_b H_{a,b}P_b(t). \tag{2.5}$$

The Hamiltonian H is an $Z(L) \times Z(L)$ intensity matrix: $H_{a,b}$ $(a \neq b)$ is nonpositive and $\sum_a H_{a,b} = 0$. $-H_{a,b}$ $(a \neq b)$ is the rate for the transition $|b\rangle \to |a\rangle$. The ground-state wavefunction of the system $|0\rangle$, $H|0\rangle = 0$, gives the probabilities in the stationary state:

$$|0\rangle = \sum_a P_a|a\rangle, \qquad P_a = \lim_{t\to\infty} P_a(t). \tag{2.6}$$

In order to go from the discrete time description of the stochastic model to the continuous time limit, we take $\Delta t = 1/(L-1)$ and

$$H_{ac} = -r_{ac}q_c \qquad (c \neq a), \tag{2.7}$$

where r_{ac} are the rates of the RPM and q_c is given by equation (2.4). The probabilities R_p do not enter in (2.5) since in the RPM when a tile hits a peak the tile is reflected and the configuration stays unchanged. Notice that through the q_cs the matrix elements of the Hamiltonian depend on the size of the system and the numbers of peaks n_c of the configurations.

As can be seen from (2.3) and (2.7), for $p < 1$ the adsorption and desorption are faster than at $p = 1$ and slower for $p > 1$. The slowing down is extreme for the substrate where $n_c = L/2$. In this case for the value $p = p_{\max} = 2(L-1)/L$ we have $q_c = 0$ and the substrate becomes an absorbing state.

In a previous paper it was shown that the PARPM is conformal invariant in the domain $0 \leq p < p_{\max}$. The following exact results, which are independent of p, are known for this domain.

The average height for large values of the size L of the system is equal to [11, 12]

$$h(L) = \frac{2}{\pi}\int_{\pi/L}^{\pi/2} \frac{\sqrt{3}}{2\pi} \ln\left(\frac{L}{\pi}\sin x\right) \mathrm{d}x + \beta \approx 0.1056 \ln L + \beta', \tag{2.8}$$

where β and β' are non-universal numbers.

The density of contact points $g(x, L)$ (x is the distance to the origin), in the finite-size scaling limit ($x \gg 1$, $L \gg 1$, but x/L fixed) is given by [13]:

$$g(x, L) = C\left(\frac{L}{\pi}\sin(\pi x/L)\right)^{-1/3}, \tag{2.9}$$

where

$$C = -\frac{\sqrt{3}}{6\pi^{5/6}}\Gamma(-1/6) = 0.753\,149\cdots. \tag{2.10}$$

The average density of minima and maxima (sites where adsorption does not take place) $\tau(L)$ has the asymptotic value:

$$\lim_{L\to\infty} \tau(L) = 3/4, \tag{2.11}$$

with non-universal corrections (depending on the value of p) of order $1/L$. We will use these results in sections 3 and 6.

J. Stat. Mech. (2011) P09030

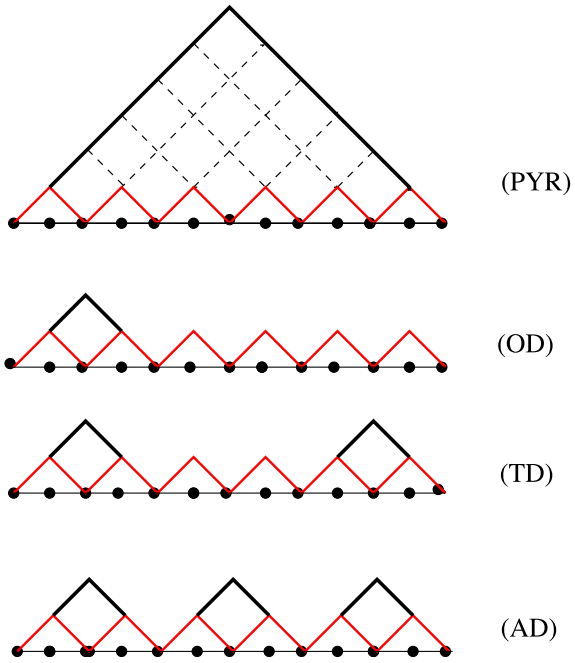

Figure 3. Special initial conditions for $L = 12$ (see text).

3. Quasistationary states at $p_{\max}$

When we understood that at $p_{\max}$ one has an absorbing state, and therefore a phase transition, we became interested in seeing how conformal invariance is broken. We expected the system to become massive, as is the usual case when conformal invariance is broken. It turns out that the new phase is a fascinating object.

We have studied several initial conditions specified by the local heights h_i (see figure 3). One is the 'pyramid' (PYR) with heights of $0, 1, 2, 3, \ldots, L/2, L/2-1, \ldots, 1, 0$. Another is the 'one dent' (OD), the heights being $0, 1, 2, 1, 0, 1, 0, 1, 0, \ldots, 1, 0$. The 'two dents' (TD) one has heights of $0, 1, 2, 1, 0, 1, 0, \ldots, 0, 1, 2, 1, 0$. The 'all dents' (AD) is defined by the local heights $0, 1, 2, 1, 0, 1, 2, 1, 0, \ldots, 0, 1, 2, 1, 0$. We have chosen these four configurations because they are extreme cases. The PYR configuration has only one peak. The OD asymmetric configuration has only one peak less than the substrate which has the maximum number of peaks. The symmetric TD configuration has two peaks less than substrate, the AD configuration is an intermediate one.

We have looked, in Monte Carlo simulations, at the average height from which we have subtracted the average height of the substrate (equal to 1/2), as a function of time taking $L = 96$, and starting with the PYR and TD initial conditions. The results of our simulations are shown in figure 4. One sees that for each of the two initial conditions one obtains time-independent results which are not zero, as one could expect to find in the absorbing state. This observation suggests the existence of QSSs [5, 6].

We have also looked at the average density of clusters $n_{cl}(t)/L$ from which we have subtracted $\frac{1}{2}$ which is the corresponding quantity for the substrate. The results for the two initial conditions PYR and TD are shown in figure 5. One obtains similar results to those shown in figure 4.

J. Stat. Mech. (2011) P09030

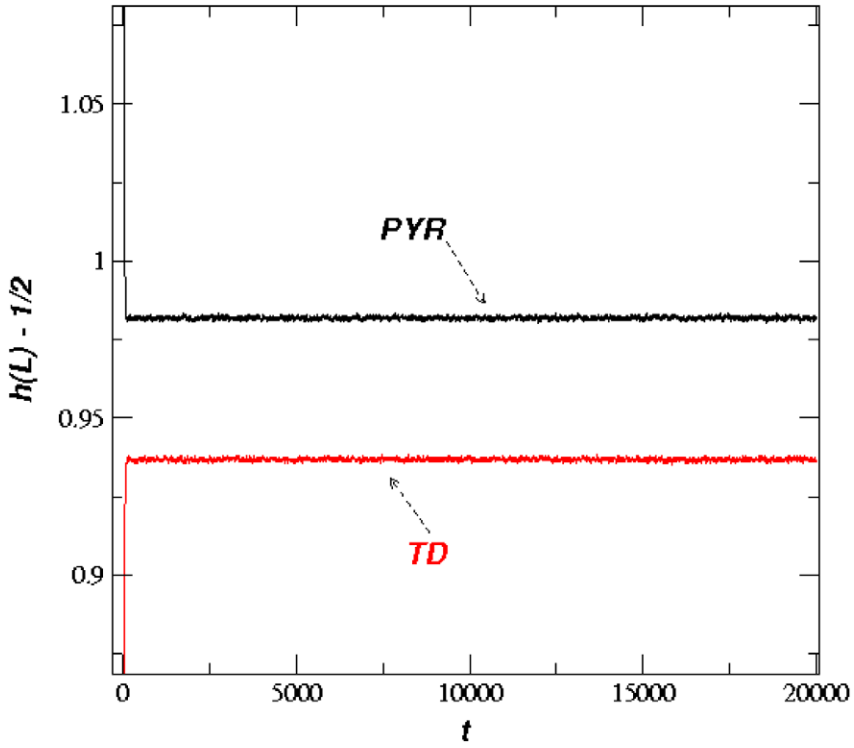

Figure 4. $p = p_{\max}$. The average height from which one has subtracted the average height of the substrate ($\frac{1}{2}$), as a function of time for two initial conditions PYR and TD. The lattice size $L = 96$. The averages are obtained taking 6×10^5 samples.

Comparison of the average heights and the density of clusters for the two initial conditions suggests that one has more clusters (therefore lower values of the average height) for the TD initial condition compared to the PYR initial condition. Therefore for $L = 96$ the two QSSs are different.

Let us make an observation. If we assume that in the QSS one has the same density of clusters as in the stationary distribution observed in the $0 \leq p < p_{\max}$ case [2], for which one has an analytical expression ($n_{cl}/L = \Gamma(1/3)\sqrt{3}/2\pi L^{1/3}$), one obtains the value -0.339 for the quantity shown in figure 5. This value is close to the value seen for the PYR initial condition. This observation will play in important role in understanding the QSS.

In order to see how the QSS appeared, we looked for another quantity which was extensively studied in the PARPM [1]. This is the average density of sites where one has a maximum or a minimum in a given configuration $\tau_{\max}(L, t)$ for $p = p_{\max}$. In the PARPM and $0 \leq p < p_{\max}$, in the large L limit one has $\tau(L, \infty) = \tau(L) = 0.75$ (for the substrate $\tau(L) = 1$).

If one starts with the TD configuration and looks at time variation of the quantity $1 - \tau_{\max}(L, t)$ for different system sizes one obtains the results shown in figure 6. We can see that for small values of $L = 46$–60 one has an exponential fall-off with time. Then an almost linear decrease in time for the values $L = 62$–76. For $L = 92$ and 96 one sees practically no time variation and a value $\tau_{\max}(L, t) \sim 0.77$ very close to the value 0.75 seen in the stationary state in the conformal invariant domain of the model. This makes

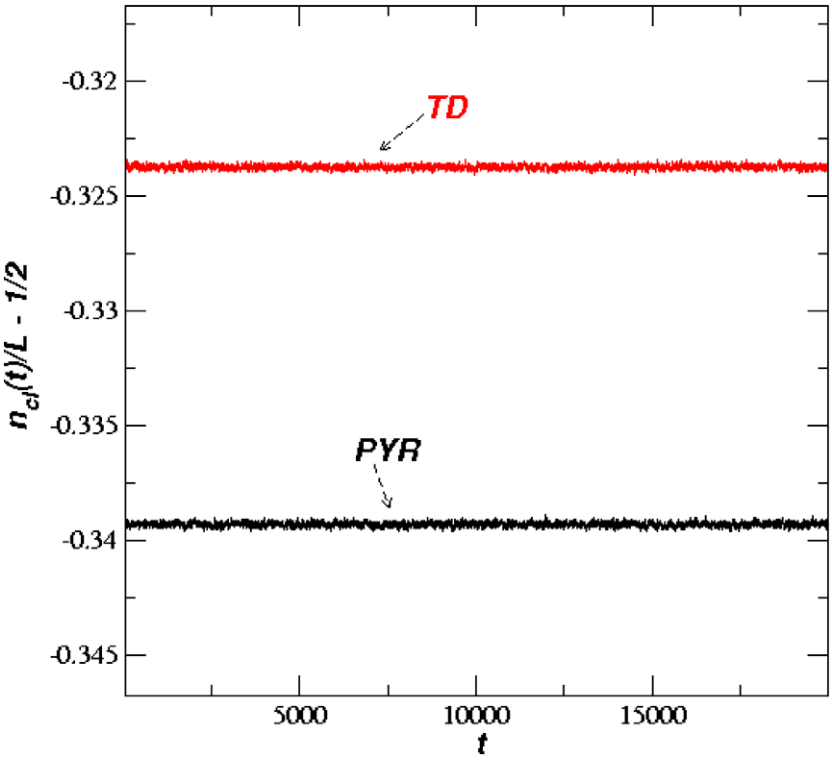

Figure 5. The density of clusters $-1/2$ (the density of clusters in the substrate) as a function of time. Same conditions as in figure 3.

us suspect the following behavior of $\tau_{\max}(L,t)$ in the QSS:

$$1-\tau_{\max}(L,t) = A(L)\exp(-E(L)t), \tag{3.1}$$

where $E(L)$ decreases exponentially with L and $A(L)$ increases smoothly with L to the value of 0.25 observed for the stationary states in the $0 \leq p < p_{\max}$ domain. In figure 7, we show for $L = 50$ the data undistinguished from a fit:

$$1-\tau_{\max}(50,t) = 0.217\exp(-0.000\,0522t). \tag{3.2}$$

Notice the very small value of E and the fact that $A(50)$ is not far from the value 0.25.

We sum up our observations; although for $p = p_{\max}$ we expected the system to relax in the absorbing state we observed the existence of states with very long relaxation times. For the lattice sizes presented above, the QSS depends slightly on the initial conditions. Surprisingly, the density of clusters and of maxima and minima in the QSS have values closed to those observed in the stationary states for $0 \leq p < p_{\max}$. Actually for the PYR initial condition the results coincide. In the next three sections we will explain these observations.

4. The spectrum and wavefunctions of the Hamiltonian. How a QSS occurs at $p_{\max}$

In order to understand the origin of the QSS we have studied the spectrum of the Hamiltonian which gives the time evolution of the system (see equation (2.5)). For

J. Stat. Mech. (2011) P09030

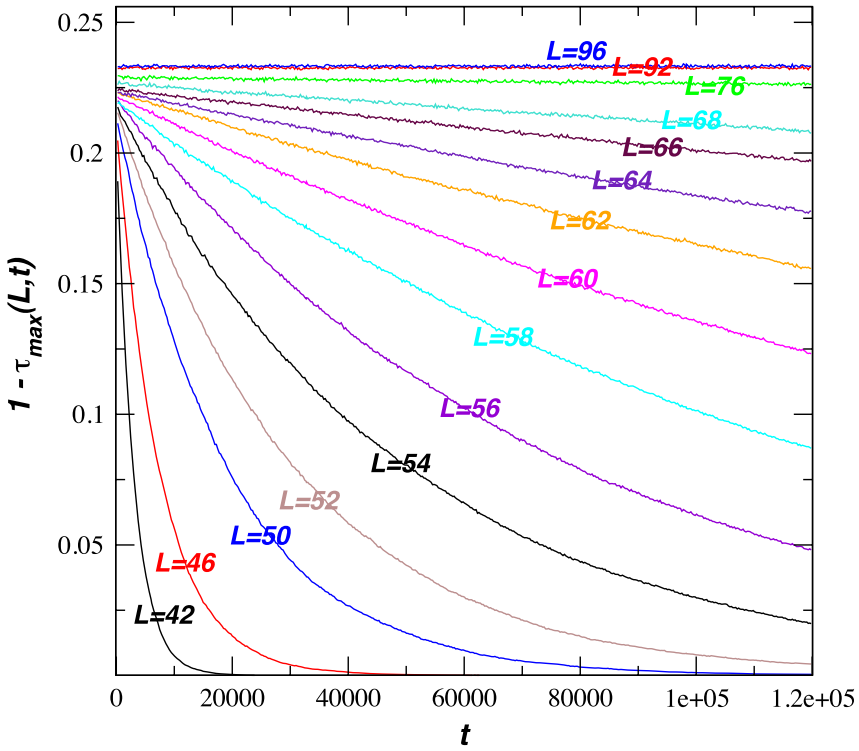

Figure 6. $p = p_{\max}$. Average density of minima and maxima $\tau_{\max}(L,t)$ subtracted from 1, as a function of time for different lattices L. The initial condition OD was chosen. The averages are obtained by taking 6×10^5 samples.

$0 \leq p < p_{\max}$, where we have conformal invariance, we have checked [1] that in the finite-size scaling limit

$$\lim_{L\to\infty} E_i(L) = \pi v_s \Delta_i / L, \qquad i = 0, 1, 2, \ldots, \tag{4.1}$$

where $E_0 = 0$, Δ_i are the scaling dimensions, and the sound velocity has the expression

$$v_s(p) = (1 - 3(p-1)/5)3\sqrt{3}/2. \tag{4.2}$$

Notice that the velocity decreases when $p > 1$ since, as described in section 2, the transition rates are smaller. The scaling dimensions are given by the partition function [4]:

$$Z(q) = \sum_{i=0}^{\infty} q^{\Delta_i} = (1-q)\prod_{n=1}^{\infty}(1-q^n)^{-1}. \tag{4.3}$$

We give the first values of Δ_is together with the corresponding degeneracies (d_is):

$$\Delta = 0(1), 2(1), 3(1), 4(2), 5(2), 6(4), 7(4), \ldots. \tag{4.4}$$

We will check whether these values will also be seen for $p = p_{\max}$.

In order to estimate the values of the Δ_is, we have taken $L = 18$ (this is not a small lattice!) and diagonalized numerically the Hamiltonian for various values of p. The results are shown in figure 8 where the first 11 levels are seen (the ground-state energy E_0 is equal to zero). The remaining 10 levels should correspond roughly (see (4.4)) to $\Delta = 2, 3, 4, 5$

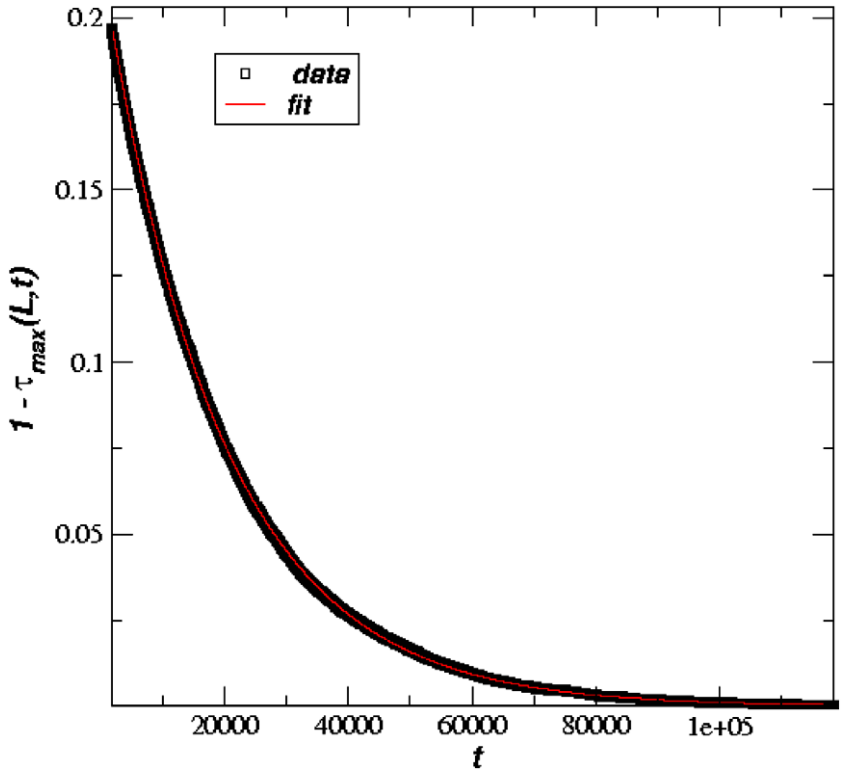

Figure 7. The average density of minima and maxima $\tau(L)$ as a function of time for $L = 50$ together with the fit (3.2). The initial configuration is OD and the averages are obtained by taking 6×10^5 samples.

and 6. We can see that for $p = 1$, where the model is integrable, this is indeed the case. The levels cluster in the right places. When p increases, one notices that the properly scaled E_1, after a smooth behavior up to $p \approx 0.9$, decreases rapidly for $p = p_{\max}$ (we have used for $v_s(p_{\max})$ the value given by (4.2) for $p = 2$). Using Monte Carlo simulations, we have checked [1] that for $p < p_{\max}$ the small decrease with p of E_1 is a finite-size effect and therefore what one sees in the figure is a crossover effect. One can also see that for increased values of p, E_4 crosses E_3 and that E_9 crosses all the levels $E_8, \ldots, E_5$. Except for the three levels E_1, E_4 and E_9 which decrease dramatically for $p = p_{\max}$, the other levels have the same finite-size behavior as those in the conformal invariant domain ($p < p_{\max}$). This suggests that the three levels mentioned above might be related to the QSS. We now proceed to a detailed analysis of these observations.

Using different lattice sizes we have computed E_1 as a function of L up to $L = 30$. For this calculation we could study larger lattices due to a special property of the Hamiltonian at $p = p_{\max}$. As we are going to show in section 5, the eigen level corresponding to E_1 is the ground-state energy of a reduced matrix defined in a basis where the absorbing state is absent. In this case, by using the power method we were able to calculate E_1 up to $L = 30$. The results can be seen in figure 9. Using the two points corresponding to the largest lattice sizes, one obtains:

$$E_1(L) = 0.912 \exp(-0.206L). \tag{4.5}$$

J. Stat. Mech. (2011) P09030

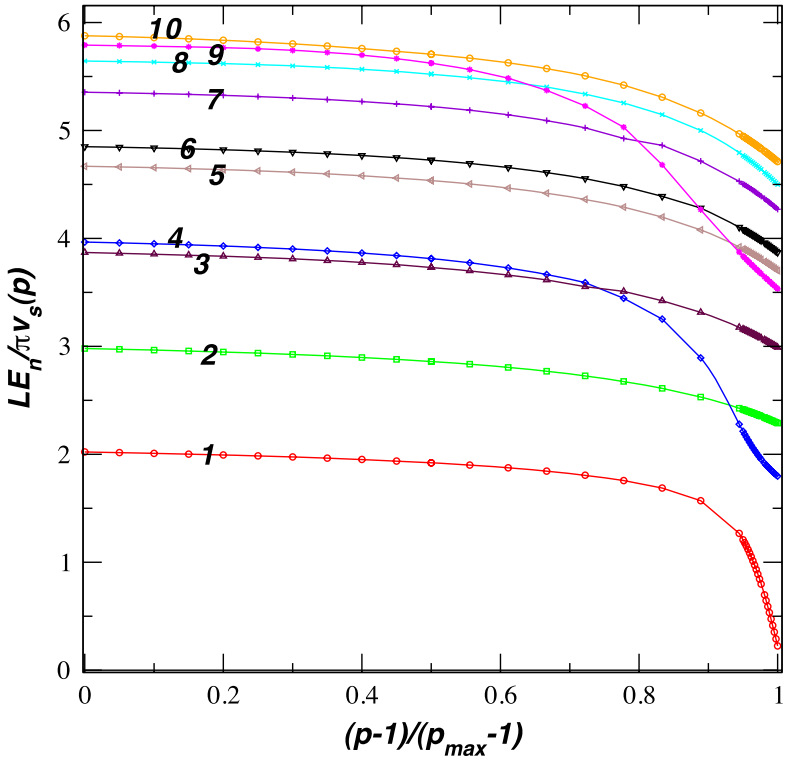

Figure 8. Estimates $\Delta_n^{(n)} = LE_n/\pi v_s(p)$ of the scaling dimensions Δ_n for different values of p, and for the lattice size $L = 18$. The estimates corresponding to the first 11 energy levels are shown. The values of $v_s(p)$ were obtained from (4.2).

To be sure that a power law behavior ($E \approx L^{-m}$) is excluded, we have estimated the derivative $-\mathrm{d}/\mathrm{d}\ln(L)\{\ln(E_1(L))\}$. This quantity should reach a constant for large values of L if $E_1(L)$ behaves as a power but should diverge linearly in the case of exponential behavior like (4.5). As seen from figure 10, the exponential behavior (4.5) is correct.

A similar analysis of $E_4(L)$ but up to $L = 18$ only, gives a similar result:

$$E_4(L) = 2.41\exp(-0.10L). \tag{4.6}$$

We have not looked at $E_9(L)$ but we expect again an exponential fall-off. We conclude that three energy levels have an exponential fall-off and that they can be related to the QSS. This will be shown to be the case in section 5. We proceed by looking at the remaining levels.

The data suggest that at $p = p_{\max}$, the energy levels that do not go exponentially to zero have the same finite-size scaling behavior as those in the conformal invariant domain. This would imply that instead of (4.4) we would have

$$\Delta = 0(1), 3(1), 4(1), 5(2), 6(3), \ldots. \tag{4.7}$$

If confirmed, this would lead us to a strange picture since the scaling dimension $\Delta = 2$ does not appear. This dimension corresponds to the energy–momentum, and therefore conformal invariance could not apply and we could not explain the finite-size behavior of the remaining levels. What can go wrong in our picture? One possibility is that the finite-size scaling of the levels doesn't satisfy (4.1).

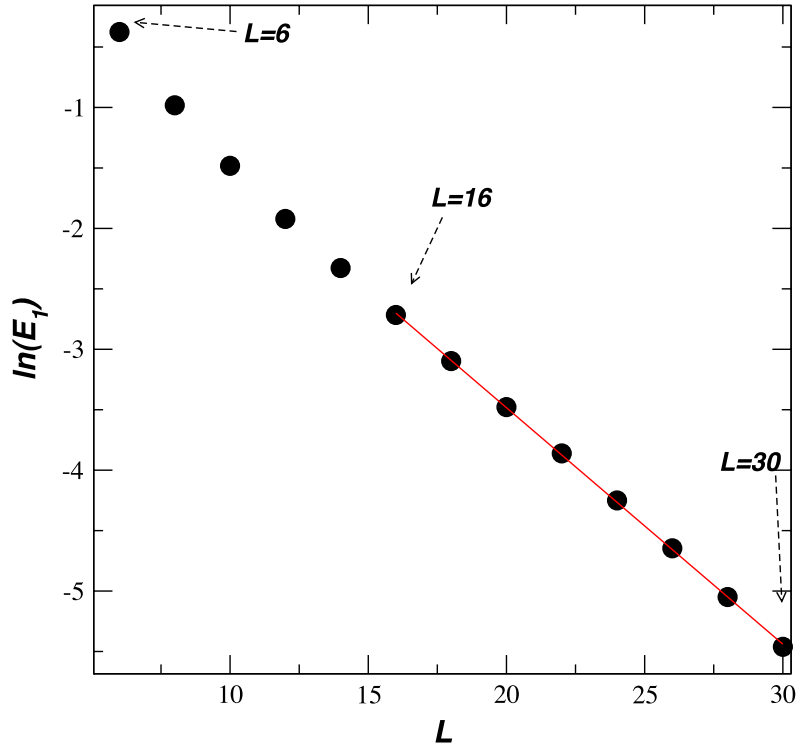

Figure 9. $\ln(E_1)$ as a function of the lattice size L for $p = p_{\max}$. The red line is a guide for the eyes, and is obtained from a fit where the lattice sizes $L = 16$–30 were used.

We have computed $E_2(L)$ up to $L = 18$. A fit to the data gives $\Delta_3 = 3.05$ in agreement with what should be expected. Similarly examining $E_4(L)$ one finds $\Delta_4 = 3.95$ also as expected. These estimates were found assuming that $v_s(p_{\max})$ is given by equation (4.2). Can we get $\Delta = 2$ by changing the sound velocity such that $E_3(L)$ gives $\Delta = 2$, $E_5(L)$ gives $\Delta = 3$, $E_6(L)$ gives $\Delta = 4, \ldots$? We have computed the ratios $E_5(L)/E_3(L)$ and $E_6(L)/E_3(L)$ as a function of L. One should obtain $4/3$, respectively $5/3$, if one had (4.3) and $3/2$, respectively 2, if the energy–momentum tensor would be present. In figures 11 and 12 we show these ratios as functions of $1/L$. Cubic fits give the values 1.32, respectively 1.64. We conclude that (4.7) is most probably correct. We have also checked that there are no energy crossings for the levels which cluster around $\Delta = 7$.

The analysis of the energy levels (compare (4.4) with (4.7)) suggests that at $p = p_{\max}$ the partition function (4.3) changes in the following way: the degeneracy at each even value of Δ decreases by one unit. Each energy level which left the Virasoro representation at non-zero even values of Δ moves to $\Delta = 0$ which becomes infinitely degenerate. This opens a problem in the representation theory of the algebra which might be solvable since the central charge is $c = 0$. In section 6 we are going to learn more about this puzzle.

5. From eigenfunctions of the Hamiltonian to QSS

We have seen in the last section that some eigenvalues of the Hamiltonian vanish exponentially. Here we will show what their connection is to QSS. In order to do so, we first prove a special property of Hamiltonians in the presence of an absorbing state.

J. Stat. Mech. (2011) P09030

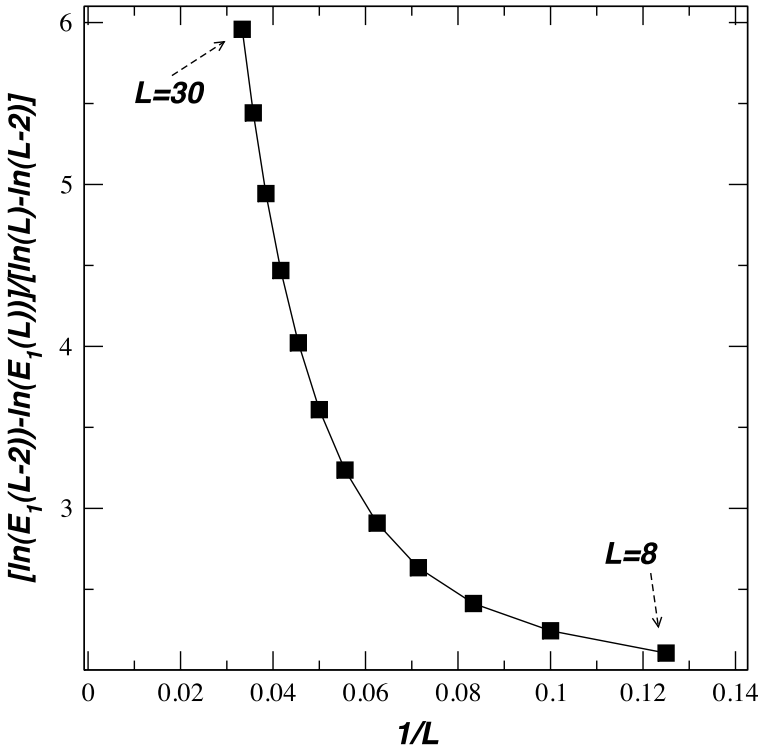

Figure 10. Estimates of $-\mathrm{d}/\ln(L)\{\ln(E_1(L))\}$ as a function of $1/L$ for different lattice sizes ($p = p_{\max}$).

We denote the vector space corresponding to $n+1$ configurations by $|0\rangle$, $|i\rangle$ ($i = 1, 2, \ldots, n$), in which we have chosen $|0\rangle$ to be the absorbing state. The Hamiltonian has the following properties:

$$H_{i,0} = 0, \qquad H_{0,0} = 0, \qquad H_{i,j} \leq 0, \tag{5.1}$$

$$H_{0,j} + \sum_i H_{i,j} = 0 \qquad (j = 1, 2, \ldots, n). \tag{5.2}$$

Assume that E_k ($k = 1, \ldots, n$) is a non-vanishing eigenvalue of H with an eigenvector $(y_0^{(k)}, y_1^{(k)}, \ldots, y_n^{(k)})$. We can show that the sum of the components of any eigenvector is equal to zero:

$$y_0^{(k)} + \sum_i y_i^{(k)} = 0 \qquad (k = 1, 2, \ldots, n). \tag{5.3}$$

Using (5.1) and (5.2) we have:

$$E_k y_0^{(k)} = \sum_i H_{0,i} y_i^{(k)} = -\sum_{j,i} H_{j,i} y_i^{(k)} = -E_k \sum_j y_j^{(k)}, \tag{5.4}$$

from which the identity (5.3) follows.

We consider now the reduced matrix $H'_{i,j} = H_{i,j}$ ($i, j = 1, 2, \ldots, n$) (the configuration $|0\rangle$ is taken out). Let E_1 be the lowest non-vanishing eigenvalue, from (5.1) and using the Perron–Frobenius theorem, we get:

$$y_i^{(1)} \geq 0, \tag{5.5}$$

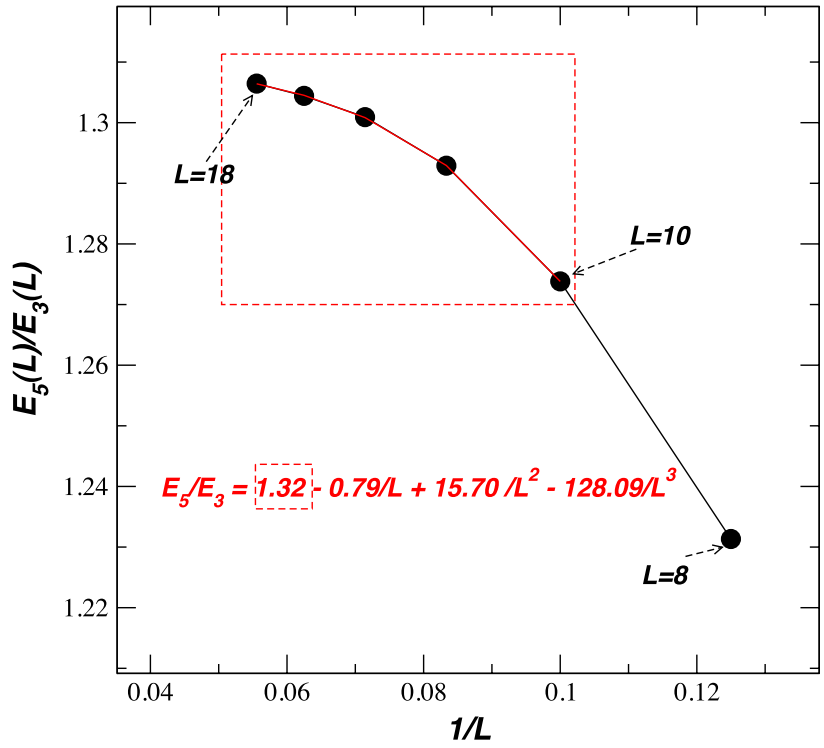

Figure 11. Ratio samong the two lowest eigenenergies, at $p = p_{\max}$, that does not vanish exponentially. The data are plotted as a function of $1/L$ for lattice sizes $L = 8$–18. A cubic fit was done by using the five largest lattice sizes.

and using (5.3), $y_0^{(1)} < 0$. From the same theorem we also learn that E_1 is the unique eigenvalue for which (5.5) occurs. For the other eigenvalues, at least one component of the wavefunction is negative, i.e. equation (5.5) is not valid for $y_i^{(k)}$ $(k > 1)$.

The solutions of the differential equation (2.5) are

$$P_0(t) = 1 + \sum_k A_k y_0^{(k)} \exp(-E_k t), \qquad P_i(t) = \sum_k A_k y_i^{(k)} \exp(-E_k t). \tag{5.6}$$

The n constants A_k are determined from the initial conditions.

At large values of L and t, the exponentially falling energies give the major contributions to $P_0(t)$ and $P_i(t)$. Among them, E_1 plays a special role. Note only is E_1 the smallest energy, but the components of its eigenfunction are positive (5.5). This implies that for a large range of L and t (both of them large), one can keep only the term with $k = 1$ in the sums appearing in (5.6). The situation is different at very large values of L when all the exponentially falling energies are practically equal to zero and more terms can appear in (5.6). Independent of the initial conditions, the term with $k = 1$ has to be present in the sums (5.6) in order to ensure the positivity of the probabilities $P_0(t)$ and $P_i(t)$, since for the other eigenfunctions (5.5) are not valid. For example, the eigenfunctions corresponding to the levels $E_4(L)$ and $E_9(L)$ of figure 8 have components with both signs in the sum giving $P_i(t)$.

We are now in a position to show how exponentially falling energies like $E_1(L)$ (see (4.5)) can be the origin of QSS. For our discussion we will assume that the term

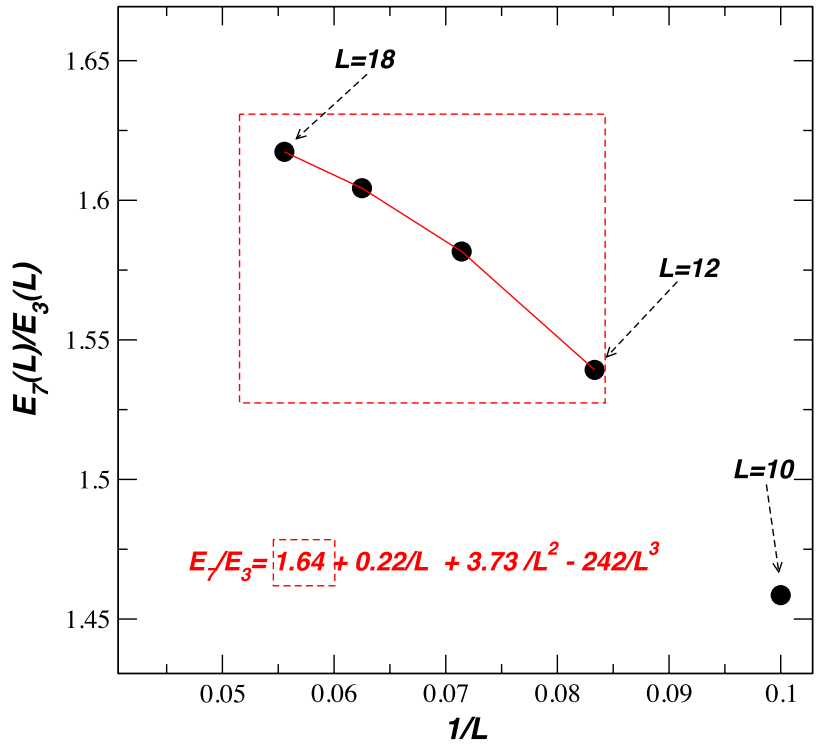

Figure 12. Ratio among the third and second lowest eigenenergies, at $p = p_{\max}$, that does not vanish exponentially. The data are plotted as a function of $1/L$, for lattice sizes $L = 10$–18. A cubic fit was done by using the four largest lattice sizes.

with $k = 1$ alone is present in (5.6). It turns out that this assumption will help to explain all the results obtained for the Monte Carlo simulations. The probability vector $|P(t, L)\rangle$ becomes:

$$|P(t, L)\rangle = [1 - a(L)\exp(-E_1(L)t)]|0\rangle + a(L)\sum_i p_i(L)|i\rangle \exp(-E_1(L)t), \tag{5.7}$$

where we have used (5.3) and (5.5)

$$a(L) = A_1 \sum_i y_i^{(1)}(L); \qquad p_i(L) = y_i^{(1)}(L) \Big/ \sum_i y_i^{(1)}(L). \tag{5.8}$$

Note that $p_i(L)$ gives the probability of finding the system in configuration $|i\rangle$ if the system is in the stationary state of the reduced Hamiltonian H', that acts in the vector space where the substrate is absent. Thus, equation (5.7) explains the occurrence of a QSS. If L is large enough, $E_1(L)$ is negligible, and one finds:

$$|P(L)\rangle = (1 - a(L))|0\rangle + a(L)|P_{\rm ns}(L)\rangle. \tag{5.9}$$

Here $a(L)$ depends on the initial conditions and it is not equal to zero. $|P_{\rm ns}(L)\rangle$ is a probability distribution function of configurations in which the substrate is not present. Equation (5.9) therefore describes the QSS. Using Monte Carlo simulations we have

measured the probability of finding the system in the substrate. For the OD initial condition (see section 3 for the definition), one finds:

$$1 - a(L) \sim 4.5/L. \tag{5.10}$$

For the PYR initial condition one finds $1 - a(L) = 10^{-5}$ for $L = 96$ (we did not compute $a(L)$ for the TD and AD initial conditions). This implies that for large values of L one has

$$|P(L)\rangle = |P_{\rm ns}(L)\rangle, \tag{5.11}$$

and the substrate does not occur in the QSS. We postpone the discussion of the results shown in figure 6 up to section 6.

6. The quasistationary states

In this section we are going to identify the QSSs observed in the Monte Carlo simulations (see figures 4–7), and find a puzzle. The basis of our identification are equations (5.7), (5.9) and (5.11).

We have taken large lattices and started our simulations with the PYR initial condition. We first looked at the average height $h(L)$. The results are shown in figure 13. The data can be fitted by a straight line. Taking only the two largest lattice sizes we obtain:

$$h(L) = 0.1068 \ln(L) + 0.042, \tag{6.1}$$

in astonishing agreement with the expression (2.8) derived [11, 12] assuming conformal invariance and used to describe the data for $0 \leq p < p_{\rm max}$. Since for the large lattices we have considered, we can use (5.11) and this would imply that $|P_{\rm ns}(L)\rangle$ is given by the same function as the one seen away from $p_{\rm max}$.

If confirmed, this result would be surprising, because as we have discussed in section 4, as compared to the conformal invariant domain, at $p = p_{\rm max}$ the finite-size spectrum of the Hamiltonian is a 'mutilated' one. It lacks not only the energy–momentum tensor but other levels too. On the other hand the space-like correlation functions look to be unaffected.

In figure 14 we show for the AD initial condition the density of contact points $g(x, L)$ for various lattice sizes divided by the finite-size scaling distribution (2.9) in the QSS. The coincidence of the $p_{\rm max}$ data and the expectation coming from conformal invariance in the QSS is astonishing (for the large lattices considered here $a(L)$ is practically equal to 1).

From now on, we will assume that for large lattices the QSS correlators are those of the conformal invariant model (RPM) and will try to explain the results described in section 3.

We use equation (5.9) and the observation that for the initial condition PYR $a(L) = 1$; taking $a(96) = 0.975$ for the TD initial condition we obtain the results for TD presented in both figures 4 and 5 (we do not have at hand an independent measurement of $a(L)$ for the TD initial condition).

We proceed by looking for a description of the data presented in figure 6, where the time dependence of the quantity $1 - \tau_{\rm max}(L, t)$, taking the OD initial condition, is

J. Stat. Mech. (2011) P09030

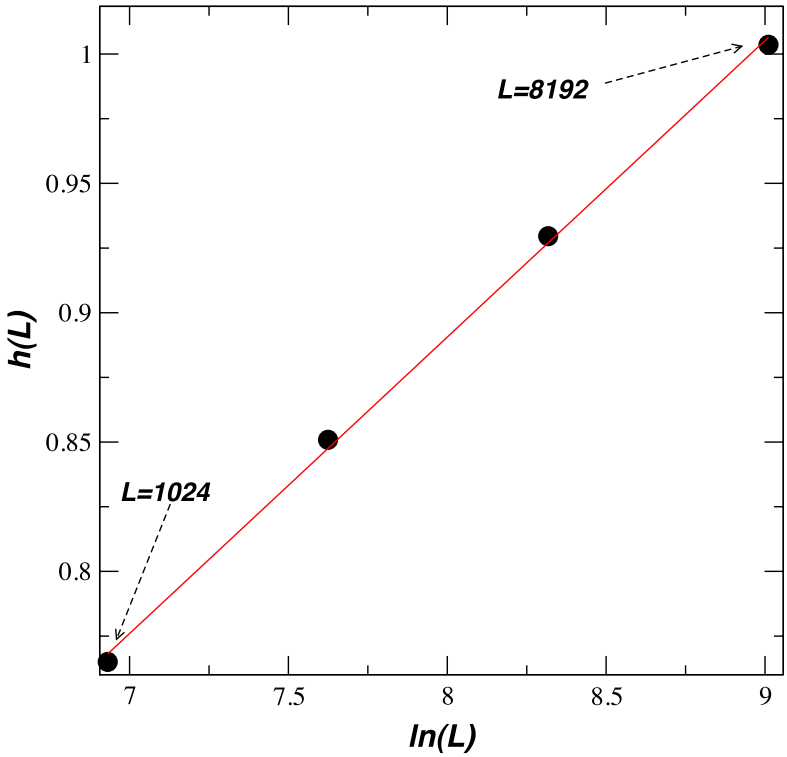

Figure 13. The average height $h(L)$ as a function of $\ln(L)$ in the QSS. $L = 1024$, 2048, 4096 and 8192. We have used PYR as an initial distribution.

shown. $\tau_{\max}(L,t)$ is the average density of minima and maxima which is equal to 1 for the substrate. We use equations (5.7) and (5.10) to get:

$$1 - \tau_{\max}(L,t) = [-4.5/L + 1 - (1 - 4.5/L)\tau(L)] \exp(-E_1(L)t). \tag{6.2}$$

The function $\tau(L)$ is known analytically only for $p = 1$ [2]. It is equal to 3/4 in the large L limit and has non-universal corrections of order $1/L$ which are unknown for $p = p_{\max}$. In principle these corrections can be determined by looking at the QSS obtained using PYR initial conditions. We can, however, use the result obtained in [1] for $p = 1.99$ where we found $\tau(L) \approx 0.75 - 0.3/L$ and use it in (6.2) to get a fair description of the data. We obtain

$$1 - \tau_{\max}(L,t) \approx (0.25 - 0.8/L) \exp(-E_1(L)t). \tag{6.3}$$

The value of $E_1(L)$ can be estimated from (4.5). In figure 15 we use this function, together with the predicted values of $E_1(L)$ given in (4.5), to compute the time dependence of $1 - \tau_{\max}(L,t)$ for the same lattice sizes used in figure 6. We can see that the overall behavior of figures 15 and 6, generated by the Monte Carlo simulations, is the same.

7. Conclusions

The parameter p which enters in the definition of the peak adjusted raise and peel stochastic model determines a domain $0 \leq p < p_{\max}$ in which one has conformal invariance.

J. Stat. Mech. (2011) P09030

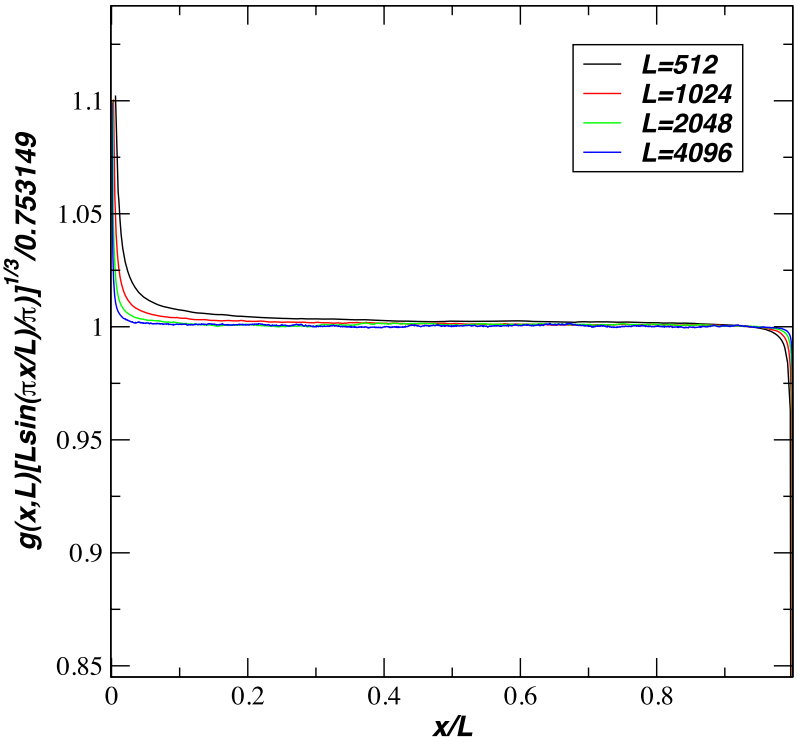

Figure 14. The density of contact points $g(x, L)$ as a function of x/L at $p_{\max}$, divided by (2.9). $L = 1024$, 2048, 4096 and 8192. Initial condition AD. The average are obtained from 3500 samples running 10^6 Monte Carlo steps.

In the finite-size scaling regime all the properties are independent on p which appears only in the sound velocity $v_s(p)$ which fixes the time scale. If $p > 1$, global properties of the configurations (the number of peaks) and the size of the system L, enter in the rates. The larger the number of peaks of a configuration, the smaller are the rates to escape the configuration. As a result, at $p = p_{\max} = 2(L-1)/L$ the configuration with the largest number of peaks, which is the substrate, becomes an absorptive state for any size of the system. Since there are no fluctuations in the ground-state of the system, we expect conformal invariance to be lost and get into a massive phase. This is not the case and a fascinating phenomenon takes place.

The new features of the model at $p = p_{\max}$ are encoded in figures 4 and 6. If the evolution of the system starts with a given initial configuration, instead of moving fast to the absorbing state, the system gets stuck in another configuration and the relaxation time grows exponentially with the size of the system. This is a QSS. In figure 8 we look at the spectrum of the Hamiltonian and follow the change of the scaled energies with increasing values of the parameter p. From the 11 energy levels shown in the figure, eight of them are those of the conformal invariant region ($0 \leq p < p_{\max}$). Three of them go exponentially to zero for large values of L.

In this paper we have tried to clarify this phenomenon. Based, unfortunately, on numerics, the following picture emerges. The wavefunction corresponding to the first excited state whose energy vanishes exponentially, gives the probability distribution function of the QSS. This is due to a peculiar property of the first excited state of

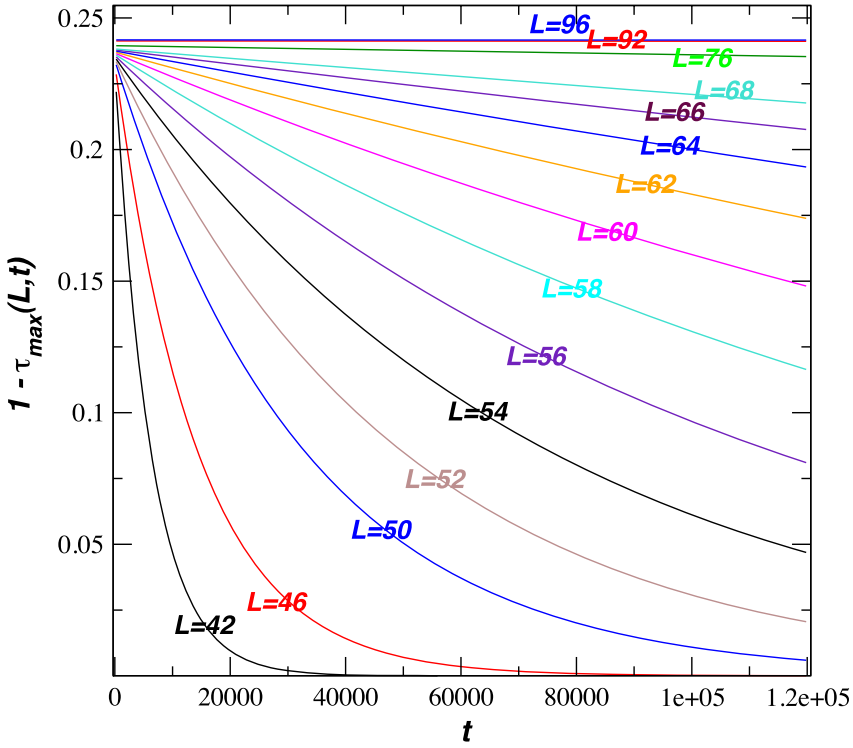

Figure 15. The average density of minima and maxima $\tau_{\max}(L,t)(L,t)$ subtracted from 1, as a function of time for the same lattice sizes L, as in figure 6. The initial condition is OD. The data were generated from the prediction (6.3), using E_1 given by (4.5).

any stochastic Hamiltonian in the presence of an absorbing state. For finite values of L, the QSS depends on the initial conditions, but in the thermodynamical limit it becomes independent of them. The ground-state observed for any finite L decouples from the system in the thermodynamic limit and is replaced by at least one of the excited states which have energies decreasing exponentially to zero for large values of L (some of these states might also decouple from the system). Unexpectedly, the finite-size scaling properties of the QSS are identical to the one observed for the ground-state in the conformal invariant domain.

This picture describes a strange way to break conformal invariance. Part of the spectrum stays unchanged (not the scaling dimension of the energy–momentum tensor!) and another part sinks in the vacuum which becomes possibly infinite degenerate. We have no idea how to explain this observation. At the same time, the space-like correlations seen in the QSS are those of the conformal domain. This is obviously an unexplained paradox. A study of space–time correlation functions should shade light in this problem. We plan to do it in the future.

We have studied only four initial conditions and found essentially only one QSS. This QSS could be related to the eigenfunction corresponding to the first excited state. It is most probable that we have missed other QSSs which should be related to some linear combination of eigenfunctions corresponding to the remaining exponentially decaying energies.

doi:10.1088/1742-5468/2011/09/P09030

The search for QSSs should continue in some extensions of the PARPM. One can look at the fate of defects like those studied in [14] when the rates are adjusted to the number of peaks. Another interesting avenue is to study the effect of changing the rates depending on the number of peaks in the extension [2, 3] of the raise and peel model in which the rates of adsorption and desorption are not equal.

Acknowledgments

We would like to thank S Ruffo, A Bovier, H Hinrichsen, J A Hoyos and P Ruelle for reading the manuscript and discussions. This work was supported in part by FAPESP and CNPq (Brazilian Agencies). Part of this work was done while VR was visiting the Weizmann Institute. VR would like to thank D Mukamel for his hospitality and the support of the Israel Science Foundation (ISF) and the Minerva Foundation with funding from the Federal German Ministry for Education and Research.

References

[1] Alcaraz F C and Rittenberg V, 2010 *J. Stat. Mech.* P12032
[2] de Gier J, Nienhuis B, Pearce P and Rittenberg V, 2004 *J. Stat. Phys.* **114** 1
[3] Alcaraz F C and Rittenberg V, 2007 *J. Stat. Mech.* P07009
[4] Read N and Saleur H, 2001 *Nucl. Phys.* B **613** 409
[5] Campa A, Dauxois T and Ruffo S, 2009 *Phys. Rep.* **480** 57
[6] Mukamel D, 2008 *Lecture Notes at Summer School in Les Houches (France)* ed T Dauxois, S Ruffo and L Cuglinadolo (Oxford: Oxford University Press) pp 4–29
[7] Gupta S and Mukamel D, 2011 *J. Stat. Mech.* P03015
[8] Politi A and Torcini A, 2010 *Nonlinear Dynamics and Chaos: Advances and Perspectives* (Heidelberg: Springer) pp 103–29
[9] Tel T and Lai Y-C, 2008 *Phys. Rep.* **460** 245
[10] Evans M R, Kafri Y, Koduvely H M and Mukamel D, 1998 *Phys. Rev.* E **58** 2764
[11] Jacobsen J L and Saleur H, 2008 *Phys. Rev. Lett.* **100** 087205
[12] Alcaraz F C and Rittenberg V, 2010 *J. Stat. Mech.* P03024
[13] Alcaraz F C, Pyatov P and Rittenberg V, 2008 *J. Stat. Mech.* P01006
[14] Alcaraz F C and Rittenberg V, 2007 *Phys. Rev.* E **75** 051110

J. Stat. Mech. (2011) P09030